

PREPARATION OF $\text{La}_{0.5}\text{Ce}_{0.5}\text{Ni}_5$ ALLOY BY ELECTRO-DEOXIDATION IN A $\text{La}_2\text{O}_3\text{-CeO}_2\text{-NiO}$ MOLTEN SALT

Q. ZHANG^{a,*}, Y. LI^{a,*}, R. SANG^a, Z. CUI^a, W. MO^b

^aAnalysis and Testing Research Centre, North China University of Science and Technology, Tangshan 063210, China

^bYisheng college, North China University of Science and Technology, Tangshan 063210, China

The $\text{La}_{0.5}\text{Ce}_{0.5}\text{Ni}_5$ alloy was successfully prepared using $\text{La}_2\text{O}_3\text{-CeO}_2\text{-NiO}$ as raw materials. The composition of cathode product was analyzed by X-ray diffractometer. The morphology of cathode and its products were observed by field emission scanning electron microscope. The product prepared by electric deoxygenation of molten salt is mainly affected by the sintering temperature and electrolytic voltage. The cathode sintered at 1050 °C is most suitable for electric deoxidation because of its suitable conductivity, particle size and pore rate, while the cathode sintered at 850 °C has poor electrical conductivity, and the cathode sintered at 1250 °C has large particle size and low stomatal ratio. In the oxide, NiO is first reduced to Ni metal, La_2O_3 reacts with CaCl_2 to form LaOCl , CeO_2 is first reduced to Ce^{3+} and then reacts with CaCl_2 to form CeOCl , and then LaOCl and CeOCl are reduced to metal on the surface of Ni under the action of Ni, then immediately react with Ni to form $\text{La}_{0.5}\text{Ce}_{0.5}\text{Ni}_5$ alloy.

(Received March 4, 2019; Accepted October 31, 2019)

Keywords: Hydrogen storage alloy, Electro-deoxidation, $\text{La}_{0.5}\text{Ce}_{0.5}\text{Ni}_5$, Molten salt

1. Introduction

Among the many categories of hydrogen storage alloys, rare earth hydrogen storage alloys (ie, AB_5 hydrogen storage alloys) are typically represented by LaNi_5 in the La-Ni alloy system. It has the characteristics of easy activation, high power discharge performance, flat P-C-T platform, and good electrocatalysis activity [1-3]. It is a type of hydrogen storage alloy with good comprehensive electrochemical performance and wide application. It has been widely used in hydrogen storage containers, hydrogen refining equipment, heat pumps and sensors, and the most successful application is as a negative electrode material for Ni-MH secondary batteries [4-6]. It has the characteristics of high specific capacity (2 times that of Ni-Cd batteries), no pollution, and long cycle life [7,8].

Willems [9] found that the initial discharge capacity of the LaNi_5 alloy can reach its theoretical capacity of 372 mA·h/g, but after 100 charge-discharge cycles, the capacity decline rate is as high as 40%, which can't meet the practical requirements of the Ni-MH battery. Until 1984,

* Corresponding author: 672219956@qq.com

Willems used cobalt to replace nickel, and a small amount of niobium to replace niobium, and a multi-alloy with high antioxidant properties was obtained. The practical Ni-MH battery was produced, and the AB₅ hydrogen storage material was re-emphasized and developed. Since then, rare earth AB₅ or AB_{5+x} hydrogen storage materials with many varieties and good performance have appeared in various countries. Among them, Rare earth elements replace A-position AB₅ hydrogen storage alloys have received much attention. Wang et al. studied the stability of the rare earth element(R) replacing the A site (A = Ca, Ce and Yb) R_{1-x}A_xNi₅ alloy and believed that it was related to the geometric and electrical factors of the alloy itself [10]. Yuan et al. studied some characteristics of the La post-system in the LaNi₅ alloy replaced by the CE part and found that with the increase of the Ce content, the sorption-desorption equilibrium pressure of the alloy increased, the thermodynamic stability decreased, and the kinetic properties increased [11]. At the same time, the doping of Ce can increase the load capacity and possible power of the alloy and reduce the discharge capacity at low discharge currents. Tan et al. studied the properties of the La_{1-x}Ce_xNi₅ (0 ≤ x ≤ 1) alloy and found that when Ce partially replaced or completely replaced La in the LaNi₅ alloy, the system storage capacity activation characteristics deteriorated. However, when the content of Ce was high, the change of Ce content has little effect on the activation characteristics of system storage capacity [12]. With the increase of Ce content, the peak discharge potential of alloy decreased. The maximum discharge capacity of the alloy is mainly related to the diffusion process of hydrogen in the system. With the increase of Ce content, the diffusion coefficient of hydrogen becomes larger. Their study also found that the LaNi₅ alloy had the highest rate of capacity ageing, while the La_{0.4}Ce_{0.6}Ni₅ alloy had the slowest rate of ageing.

In addition, we found that in these studies, the alloy materials were prepared by some traditional metallurgical methods. It is rare to report that La_{1-x}Ce_xNi₅ ternary alloys were prepared by molten salt electric deoxidation method. In this paper, we propose to prepare La_{0.5}Ce_{0.5}Ni₅ alloy by electric deoxygenation of molten salt, and study the effects of sintering temperature, electrolysis voltage, electrolysis time and other factors in preparing La_{0.5}Ce_{0.5}Ni₅ alloy by electric deoxygenation of molten salt, and discuss the reaction mechanism.

2. Experimental

The original raw materials used in the experiment were La₂O₃, CeO₂ and NiO. According to the ratio of La, Ce, and Ni atoms to 0.5: 0.5: 5, the corresponding mass of metal oxides La₂O₃, CeO₂ and NiO are weighed with a total weight of 30 g, and 1 wt %-1.5 wt % of PVB (polyvinyl butyl) is added as a binder, add an appropriate amount of ethanol, place it in a PTFE ball grinder, then place it in a planetary ball grinder and wet it for 4 h. After the ball grinder is completed, it is naturally dried in the air. The resulting powder is ground and granulated, weighed 2.5 g. press the powder into Φ20 body with the thickness is 2-3 mm under 20 MPa, and the round hole of Φ2 is drilled in the center of the specimen for use in connecting with the wire after sintering. The pressed specimen was placed near the thermocouple in the Mafulu, sintered for 4 h at 850 °C, 1050 °C, and 1250 °C, respectively, and finally cooled to room temperature.

The composition of the product was analyzed using an X-ray diffractometer(XRD, RIGAKU D/MAX 2500V/PC, Japan), and the microscopic morphology of the electric deoxygenation product was observed by field emission scanning electron microscopy (SEM,

Hitachi s4800). After sintering, the porosity of the cathode was determined by liquid static weighing method based on the Archimedes principle.

3. Results and discussions

3.1. Effect of sintering temperature on the electrolytic products

Fig. 1 shows the changes in the apparent porosity and apparent density of the specimen after sintering. It can be seen from the figure that the porosity of the specimen decreases with the increase of the sintering temperature and the apparent density increases with the increase of the sintering temperature. The porosity ratio decreased from 40.01 % at 850 °C to 37.91% at 1050 °C. The change was relatively small. However, when the temperature increased to 1250 °C, the porosity rate decreased to 12.72%, the decrease was very large, indicating that the cathode sample is relatively dense at this temperature. The same conclusion is also found in the analysis of the SEM map below. Therefore, the higher the sintering temperature, the denser the cathode and the lower the porosity.

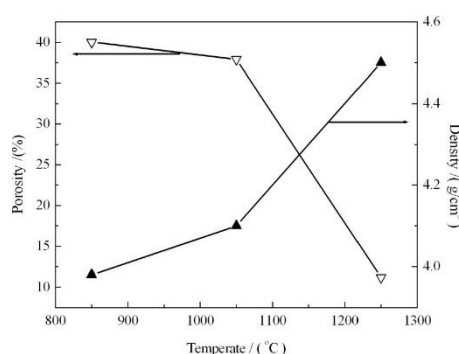


Fig. 1. Porosity and density of pellets sintered at different temperatures.

Fig. 2 shows the XRD patterns of the specimen at different temperatures. It can be seen from the figure that after sintering at 850 °C, the cathode specimen did not contain the diffraction peak of La_2O_3 , indicating that La_2O_3 had all reacted with NiO to form LaNiO_3 . At this time, CeO_2 has not reacted with NiO, indicating that the two oxides are relatively stable at this temperature. The phases contained in the specimen are: LaNiO_3 , CeO_2 , NiO. With the sintering temperature increasing to 1050 °C, the Ni element in the cathode sample had only the diffracted peaks of the two substances NiO and LaNiO_3 , indicating that La_2O_3 and NiO reacted to form LaNiO_3 at this time. The remaining NiO still exists. In addition, it can be found that CeO_2 has a decomposition reaction at this temperature, with a low oxide Ce_4O_7 generation, but at this time the temperature is low, the reaction time is short, CeO_2 decomposition is incomplete, and the remaining part CeO_2 . At this sintering temperature, the sample contains the following phases: LaNiO_3 , CeO_2 , Ce_4O_7 and NiO. After sintering at 1250 °C, only LaNiO_3 , Ce_4O_7 , and NiO were present in the cathode sample, CeO_2 was completely decomposed into Ce_4O_7 , and there was no other change in NiO that did not participate in the reaction.

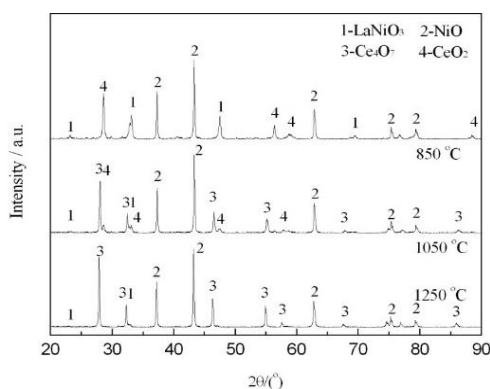


Fig. 2. XRD patterns of the pellets sintered at different temperatures for 4 h.

Fig. 3 shows the SEM morphology of the surface and section for the cathode specimen. After sintering at 850 °C, the particle spacing of the specimen surface is relatively large, the structure appears loose, and there are obvious stomata connected inside the specimen. The cross-section particles are relatively small and basically circular. When they are connected to each other, the contact area is relatively small. The gaps between the particles are many and relatively loose, and the air holes are connected to each other. Such a structure can reduce the resistance inside the sample and facilitate the molten salt entry. The reaction area during electrolysis was increased to promote the electrodeoxidation reaction. However, due to the insufficient density of the sample, the contact area between the particles is small and not close enough, and the conductive properties of the sample are relatively poor, resulting in low efficiency in electrolysis and affecting the speed of electrodeoxidation. After the cathode specimen is sintered at 1050 °C, the surface is relatively dense. Compared with 850 °C, the gap between the particles becomes smaller, the contact is closer, and the stomata are also reduced in a certain number. The particle size of most of the particles in the section increased greatly, the shape was irregular, the contact area between the particles was relatively large, and the number of stomata decreased, but the diameter of stomata increased. After sintering at 1250 °C, it can be observed from the surface that the specimen density is quite high, the grain particle size increases significantly, and there are few stomata in close contact with each other. The grains of the section accumulate closely with each other, the particle size increases, and the stomata are very few. In this case, the close contact between grains helps to increase the conductivity of the cathode and promote the electrical deoxidation reaction. However, due to the relatively large grain size, the diffusion of O^{2-} from the inside to the surface is very difficult, which will seriously slow down the entire electrical deoxidation process [13]. At the same time, there are few stomata, and the contact area between the molten salt and the sample is greatly reduced, which reduces the reaction area and slows down the speed of the electric deoxidation reaction.

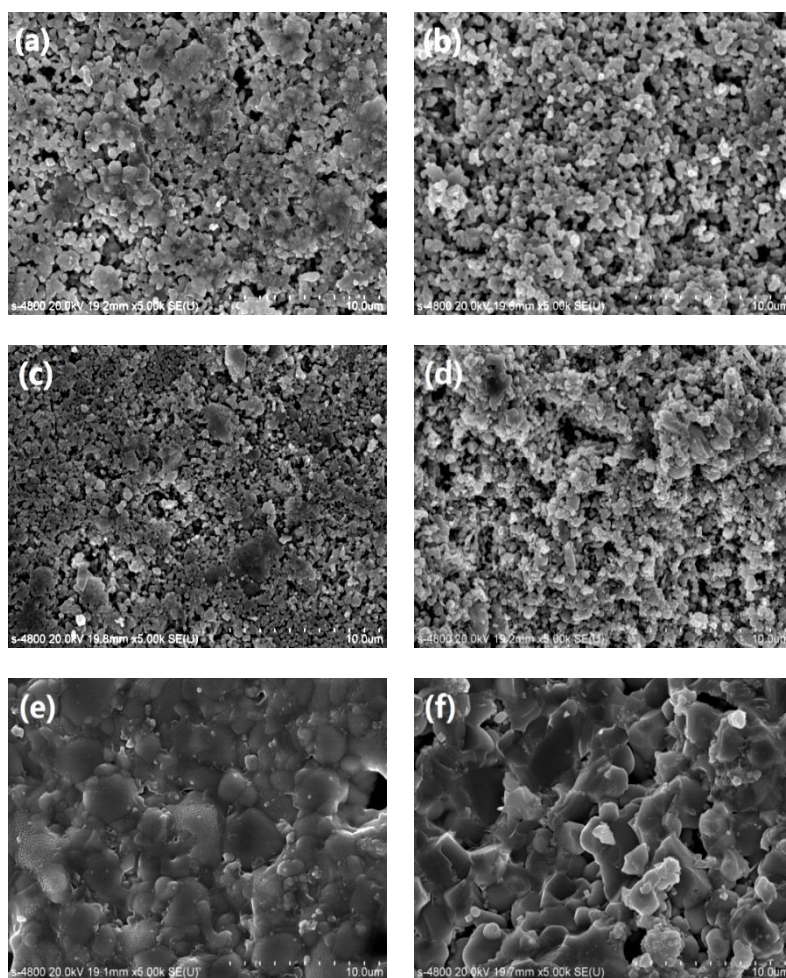


Fig. 3. SEM images of the pellets sintered at different temperatures for 4 h; (a) surface for 850 °C; (b) fracture surface for 850 °C; (c) surface for 1050 °C; (d) fracture surface 1050 °C; (e) surface for 1250 °C; (f) fracture surface 1250 °C.

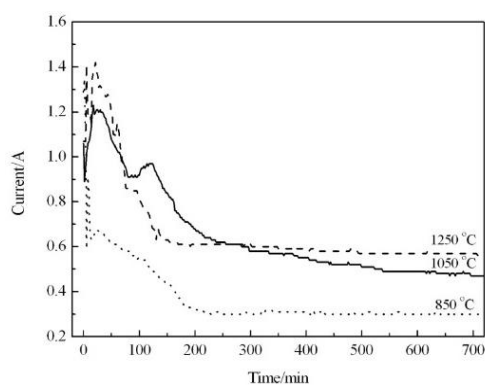


Fig. 4. Time-current plots of electrolysis production of the pellets sintered at different temperatures.

Fig. 4 shows the current-time curve of the cathode sample at 3.1 V electrolytic voltage at 12 h. In the first stage, because the deoxidation reaction is carried out on the cathode surface, the

O^{2-} diffusion speed is very high, and the molten salt is in direct contact with the cathode, therefore, neither the size of the particle nor the stomata will hinder the electric deoxidation reaction. The main factor affecting the current of electrolysis is the conductivity of the sample. The cathode electrolysis current of 1250 °C sintered was the largest, followed by the cathode of 1050 °C sintered, and the cathode of 850 °C sintered was the smallest, and the result is also consistent with the previous analysis. In the second stage, the cathode electrolysis current of 1050 °C sintered was the largest, followed by the cathode of 1250 °C sintered, and the cathode of 850 °C sintered was the smallest. It can be seen from Figure 3 that the cathode grains sintered at 1250 °C have large particle size, tight binding, and low stomatal rate. The diffusion of O^{2-} must go through a long path to reach the interface between the grains and the molten salt. The speed of the electrodeoxidation reaction is very slow. The current is relatively small during electrolysis. The cathode sintered at 850 °C has loose grains, poor electrical conductivity, and small electrolytic current. The cathode sintered at 1050 °C has a suitable size of grains and pores, so its conductivity is also relatively best, and the current is the largest during electrolysis. In the third stage, the cathode electrolysis current sintered at 1050 °C is in the middle position, less than 1250 °C and greater than 850 °C. Combined with the analysis of Figure 3, the electrodeoxidation reaction of the cathode sintered at 1050 °C has been basically completed. The cathode sintered at 1250 °C and 850 °C has not yet been completed due to the slow reaction speed, so the cathode electrolysis current sintered at 1050 °C is relatively low.

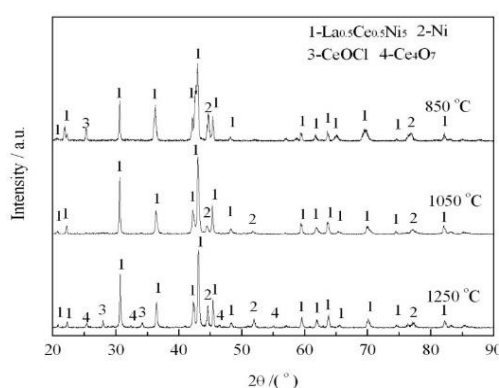


Fig. 5. XRD patterns of the electrolysis products of the pellets sintered at different temperature electrolyzed at 3.1 V for 12 h.

Fig. 5 shows the XRD map of samples sintered at three different temperatures at a constant pressure electrolysis of 12 h at a voltage of 3.1 V. It can be seen from the figure that the main components of the cathode sintered at 850 °C after 12 h electrolysis are $La_{0.5}Ce_{0.5}Ni_5$ and a small amount of Ni and CeOCl, indicating that the electrodeoxidation process has not yet been completed. The main reason is that the binding between oxide particles is not close enough, the effect of the connection is not very good, the electron transfer is slow, the reduction reaction is limited, and the deoxidation reaction is not complete enough. After the electrolysis of the cathode sintered at 1050 °C, it was all reduced to $La_{0.5}Ce_{0.5}Ni_5$. Only a small amount of Ni element existed, probably due to the fact that a small part of the intermediate product LaOCl and CeOCl dissolved in the molten salt caused Ni to be excessive. After the cathode electrolysis at 1250 °C was sintered,

in addition to $\text{La}_{0.5}\text{Ce}_{0.5}\text{Ni}_5$, there were also a small amount of Ni and the unreduced CeOCl and Ce_4O_7 . There were incomplete reactions in the sintered cathode at 850 °C and 1250 °C. Due to the high sintering temperature, the cathode sintered at 1250 °C formed a large number of closed pores. The internal particles could not come into contact with the molten salt, the reaction area was greatly reduced, and the particles were also relatively large. The diffusion path of O^{2-} ions from the interior to the surface was relatively long, its diffusion speed is relatively slow, so the cathode can't completely react. The cathode sintered at 1050 °C can completely react due to the good effect of the connection between the cathode particles, which is conducive to the conduction of electrons. The porosity is relatively large, which increases the reaction area. The particle size of a single particle is relatively small, and O^{2-} diffuses from the inside to the surface is relatively easy. This is consistent with the results of the previous microstructural analysis.

Fig. 6 shows the SEM of the sample sintered at 3.1 V voltage at 12 h. It can be seen from the figure that the structure of the cathode after electrolysis is very loose and the particles are small, and this is due to the small size of the cathode itself, which is changed from oxide to metal after electrolysis and is caused by volume contraction. After the cathode electrolysis at 1050 °C was sintered, the particles were uniform, the particle size increased significantly compared with the sample at 850 °C, and the particles were uniform in size and connected to each other. The cathode sintered at 1250 °C is large but not very uniform after electrolysis. It can also be found that the size of the particles after electrolysis is directly related to the particle size of the cathode before electrolysis, the larger the particle size before electrolysis, the larger the particle size after electrolysis.

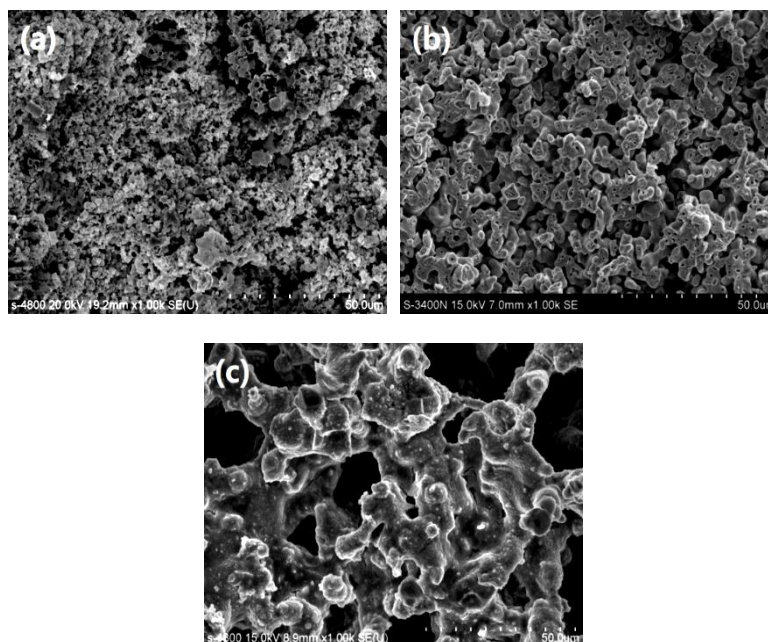


Fig. 6. SEM images of the electrolysis products of the pellets sintered at different temperature electrolyzed at 3.1 V for 12 h (a)850 °C; (b)1050 °C; (c)1250 °C.

3.2. Effect of electrolytic voltage on the electrolytic products

Fig. 7 shows the time-current curve of the cathode sintered at 1050 °C at different electrolytic voltages. From the figure, it can be clearly seen that the higher the voltage, the greater the current during electrolysis.

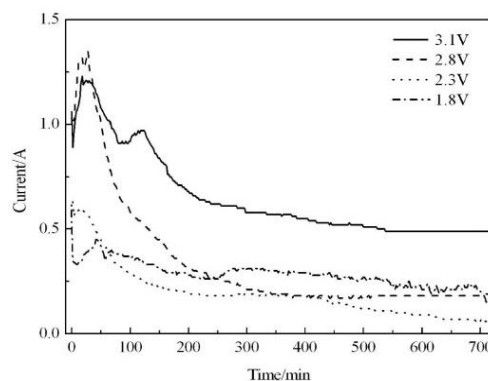


Fig. 7. Time-current plots of the pellets at different constant voltages.

The reason is roughly that under the high voltage, the electric field strength is very strong, the electromigration speed of the O^{2-} ion is very large, the O^{2-} ions in the molten salt can quickly migrate from the cathode to the anode, which reduced the O^{2-} ion concentration in the molten salt at the cathode, accordingly the concentration difference of O^{2-} ions inside and outside the cathode was increased, so the O^{2-} diffusion speed inside the cathode is accelerated, which promoted the electrical deoxidation reaction, then the electrolysis current became large [14].

After electrolyzed for 12 h at different voltages, the XRD patterns of the product are shown in Fig. 8. It can be seen from the figure that after electrolysis under 3.1 V, the sample is completely reduced, the majority of them are $La_{0.5}Ce_{0.5}Ni_5$ alloys, and the small part is the Ni metal, there is no residue of unreacted oxides and intermediates. After electrolyzed at 2.8 V, it can be found that most of the samples were $La_{0.5}Ce_{0.5}Ni_5$ alloys, and a small amount of Ni, as well as $CeOCl$ and Ce_7O_{12} that could not be fully reacted exist. After electrolyzed at 2.3 V, most of the NiO in the sample has been reduced to Ni metal, a small amount of NiO, and part of Ce_4O_7 is reduced and reacts with $CaCl_2$ to form $CeOCl$, because the electrolytic voltage is lower than the theoretical decomposition voltage of La_2O_3 , La_2O_3 is not restored, but reacts with $CaCl_2$ to generate $LaOCl$ with no other changes. In 1.8 V electrolysis, since the voltage is just above the theoretical decomposition voltage of NiO, most of the NiO in the sample can be reduced to Ni, and part of La_2O_3 reacts with $CaCl_2$ at high temperature to produce $LaOCl$. Ce_4O_7 does not change. It shows that alloys can't be generated below the theoretical decomposition voltage of a certain component. When the electrolytic voltage is higher than the theoretical decomposition voltage of all components, alloys can be generated, and as can be seen from Fig. 7, the higher the voltage, the faster the electrical deoxidation reaction. Therefore, the optimized electrolytic voltage selected in the experiment is 3.1 V, which can not only obtain pure alloys, but also enable the reaction to be completed quickly.

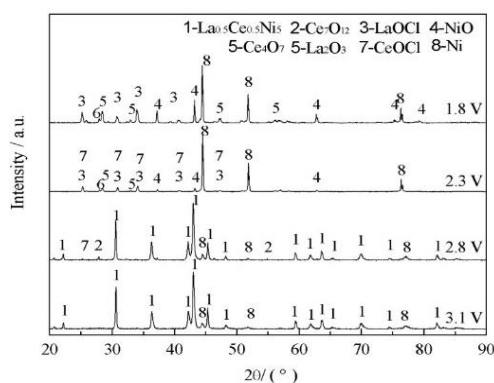


Fig. 8. XRD patterns of the electrolysis products of the pellets sintered at 1050 °C electrolyzed at different voltages for 12 h; (a) 1.8 V; (b) 2.3 V; (c) 2.8 V; (d) 3.1 V.

After the cathodes were sintered at 1050 °C, they were electrolyzed at 3.1 V and 2.8 V for 12 h, respectively and Fig. 9 is their SEM images. It can be clearly observed from the figure that the diameter of the product particles is relatively large at 3.1 V electrolytic voltage, the size of the particles is about 5 μm , there are holes of different sizes in the middle of the particles, and the particles are connected to each other. The diameter of the product particles at the electrolytic voltage of 2.8V is small, only about 2 μm , there are no holes in the middle of the particles, and the gap around the particles is relatively large. At 3.1 V electrolytic voltage, the reaction speed is high, so that the surface of the particles rapidly forms a metal shell and is continuously thickened. The shell can't contract in time so that a hole appears in the middle of the particles of the product, and at a lower electrolytic voltage, since the speed of the reaction is relatively slow, the speed of contraction of the shell can be synchronized with the speed of the electric deoxidation reaction, so the particles remain complete.

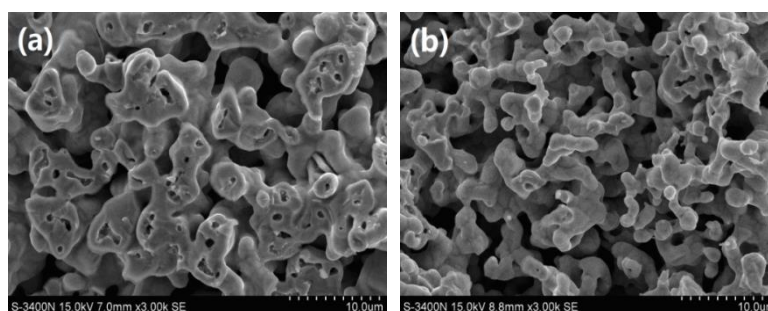


Fig. 9. SEM images of the pellets electrolyzed at different voltages for 12 h (a) 3.1 V; (b) 2.8 V.

4. Conclusions

The $\text{La}_{0.5}\text{Ce}_{0.5}\text{Ni}_5$ alloy was successfully prepared using La_2O_3 - CeO_2 -NiO as raw materials. The composition of cathode product was analyzed by X-ray diffractometer. The morphology of

cathode and its products were observed by field emission scanning electron microscope. The product prepared by electric deoxygenation of molten salt is mainly affected by the sintering temperature and electrolytic voltage. The higher the sintering temperature, the higher the grain size of the cathode and the lower the porosity, these changes of the cathode will have a direct impact on the electrodeoxidation process. The cathode sintered at 1050 °C is most suitable for electric deoxidation because of its suitable conductivity, particle size and pore rate, while the cathode sintered at 850 °C has poor electrical conductivity, and the cathode sintered at 1250 °C has large particle size and low stomatal ratio. The electric deoxidation reaction starts from the cathode surface and gradually proceeds to the inside of the cathode. NiO is first reduced to Ni metal, La_2O_3 reacts with CaCl_2 to form LaOCl, CeO_2 is first reduced to Ce^{3+} and then reacts with CaCl_2 to form CeOCl, and then LaOCl and CeOCl are reduced to metal on the surface of Ni under the action of Ni, then immediately react with Ni to form $\text{La}_{0.5}\text{Ce}_{0.5}\text{Ni}_5$ alloy.

Acknowledgements

This work is partially supported by the National Natural Science Foundation of China (Grant No. 51874137) and the Natural Science Foundation of Hebei Province (Grant No. E2017209223).

References

- [1] G. Liang, J. Huot, R. Schulz, *Journal of alloys and compounds* **320**, 133 (2001).
- [2] P. Termsuksawada, S. Niyomsoana, B. Mishraa, et al, *Materials and science and engineering B* **117**, 45 (2005).
- [3] M. Karwowska, T. Jaron, K. J. Fijalkowski et al., *Journal of Power Sources* **263**, 304 (2014).
- [4] X. X. Yan, Z. F. Ma, Y. N. Nuli, et al., *Journal of alloys and compounds* **385**(1-2), 90 (2004).
- [5] K. Panwar, S. Srivastava, *International Journal of Hydrogen Energy* **43**(24), 11079 (2018).
- [6] M. Karwowska, K. J. Fijalkowski, A. Czerwiński, *Electrochimica Acta* **252**, 381 (2017).
- [7] W. H. Zhou, Z. Y. Tang, D. Zhu, *Journal of Alloys and Compounds* **692**, 364 (2017).
- [8] W. H. Zhou, D. Zhu, K. Liu, *International Journal of Hydrogen Energy* **43**(46), 21464 (2018).
- [9] J. J. G. Willems, K. H. J. Buschow, *Journal of the less common metals* **129**(15), 13 (1987).
- [10] X. H. Wang, C. Y. Wang, C. P. Chen et al., *Journal of alloys and compounds* **420**, 107 (2006).
- [11] X. X. Yuan, H. S. Liu, Z. F. Ma et al., *Journal of alloys and compounds* **359**, 300 (2003).
- [12] Z. X. Tan, Y. F. Yang, Y. Li et al., *Journal of alloys and compounds* **453**, 79 (2008).
- [13] B. P. Tarasov, M. S. Bocharnikov, Y. B. Yanenko et al., *International Journal of Hydrogen Energy* **43**(9), 4415 (2018).
- [14] Y. Deng, D. H. Wang, G. Z. Chen, *Journal of Physics Chemistry B* **109**, 14043 (2005).